FINAL TECHNICAL REPORT

USGS AWARD G10AP00031

Studying fault friction properties based on observations of small repeating earthquakes

Principal Investigator: Nadia Lapusta, California Institute of Technology
1200 E. California Blvd., Pasadena, CA 91125
(626) 395-2277, Fax: (626) 568-2719, lapusta@caltech.edu

Abstract

Small repeating earthquakes have been discovered on a number of faults, including the Parkfield section of the San Andreas fault. Parkfield is a well-instrumented natural laboratory that displays the full range of fault slip behaviors: relatively large, M6, events, small repeating earthquakes, seismic tremors, and creeping regions. The uniqueness of this area has been exploited in a number of studies, including the San Andreas Fault Observatory at Depth (SAFOD) drilling project. Small repeating earthquakes are used to address an increasingly richer array of problems, from fault creeping velocities and postseismic slip to earthquake interaction and stress drops.

In this project, we have used the rate-and-state model for the small repeating earthquakes developed in earlier USGS-supported projects to investigate what the behavior of the repeaters can reveal about fault properties, and in particular about fault friction properties.

We have also shown that our model is capable of reproducing the non-trivial response of small repeating earthquakes to accelerated loading due to postseismic slip after the 2004 M6 event. Observations point to systematic changes in seismic moment, with some sequences experiencing significant increase in seismic moment due to higher loading rates (and hence shorter recurrence times), while other sequences have a small decrease. We find that the increase in seismic moment due to shorter recurrence times can be attributed to larger rupture area. This behavior occurs in our model for patch sizes only slightly larger than the nucleation size, suggesting that many repeating sequences at Parkfield have this property.

One of the most exciting findings is that enhanced co-seismic weakening is needed to match the relatively high stress drops of two of the SAFOD targets, the Los Angeles (LA) and San Francisco (SF) repeating sequences. To match their stress drops, we added flash heating to our model, the form of co-seismic weakening caused by rapid weakening of the tips of the frictional contacts during fast, co-seismic slip rates. The finding that flash heating may be acting in earthquakes as small as M2 is consistent with the theoretical prediction that flash heating should occur over slip scales comparable to the asperity scales of several microns, as well as with experimental trends observed for increasing normal confinement. As part of our study of the LA and SF repeaters, we have started to investigate interaction between nearby repeating sequences, and we find complex behaviors such as seismic events on sub-critical patches and quiescence of patches that would seismic in isolation.

From a more general point of view, the study has advanced our understanding of the applicability of co-seismic weakening to earthquake source processes and partition of slip into seismic and aseismic parts and their interaction. The results and the developed methodology can be applied to other problems in earthquake science. The resulting better understanding of fault physics will contribute to reduction of losses from earthquakes in the US.

Publications supported by this project:

Chen, K. H., R. Bürgmann, R. M. Nadeau, T. Chen, and N. Lapusta, Postseismic variations in seismic moment and recurrence interval of repeating earthquakes, *Earth Planet. Sci. Lett.*, 299, doi:10.1016/j.epsl.2010.08.027, 118–125, 2010.

Noda, H., and N. Lapusta, Three-dimensional earthquake sequence simulations with evolving temperature and pore pressure due to shear heating: Effect of heterogeneous hydraulic diffusivity, *J. Geophys. Res.*, 115, B12314, doi:10.1029/2010JB007780, 2010.

Chen, T. and N. Lapusta, On behavior of small repeating earthquakes in rate and state fault models, to be submitted to *Geophys. J. Int.* , 2011.

Chen, T. and N. Lapusta, Characteristics of the SAFOD target sequences explained by modeling with enhanced dynamic weakening, manuscript in preparation, 2011.

Model of small repeating earthquakes based on rate and state friction

Small repeating earthquakes occur on a number of faults and their observations have been used to study various aspects of earthquake physics and mechanics (e.g., Ellsworth and Dietz, 1990; Vidale et al., 1994; Marone et al., 1995; Nadeau and Johnson, 1998; Nadeau and McEvilly, 1999; Bürgmann et al., 2000; Beeler et al., 2001; Sammis and Rice, 2001; Igarashi et al., 2003; Imanishi et al., 2004; Nadeau et al., 2004; Schaff et al., 2004; Matsubara et al., 2005; Allmann and Shearer, 2007; Chen et al., 2007; Dreger et al., 2007). Because of their short recurrence times and known location, small repeating earthquakes present a rare predictable opportunity for detailed observation and study, and that has been exploited in San Andreas Fault Observatory at Depth (SAFOD) drilling project (e.g., Hickman et al., 2004; Imanishi et al., 2004, Zoback et al., 2010).

The model that we have considered so far for the occurrence of small repeating earthquakes contains one or more homogeneous seismogenic patches surrounded by a much larger homogeneous creeping fault zone (Figure 1; Chen and Lapusta, 2009; Chen et al., 2010) and imbedded into an elastic medium. Outside of the creeping zone, sliding with the loading rate V_L is imposed on the fault to represent the effect of the surrounding steadily creeping segment. The seismogenic and creeping parts of the fault are modeled by rate and state friction laws.

Several levels of complexity can be adopted in the description of fault friction. Our previous studies supported by USGS have shown that the standard logarithmic rate and state formulations (e.g., Dieterich, 1979, 1981; Ruina, 1983) already allow us to match a number of basic observations as discussed in section 2.2 Such laws express the dependence of frictional shear strength τ_f on the effective normal stress $\bar{\sigma}$, slip rate V (which we also call slip velocity), and evolving properties (state) of the contact population represented by the state variable θ, through:

$$\tau_f = \bar{\sigma} f = (\sigma - p)[f_o + a\ln(V/V_o) + b\ln(V_o\theta/L)],$$
$$\frac{\partial\theta}{\partial t} = 1 - \frac{V\theta}{L} \text{ or } \frac{\partial\theta}{\partial t} = -\frac{V\theta}{L}\ln\frac{V\theta}{L} \text{ or } \frac{\partial\theta}{\partial t} = \exp\left(-\frac{V}{V_c}\right) - \frac{V\theta}{L}\ln\frac{V\theta}{L}, \quad (1)$$

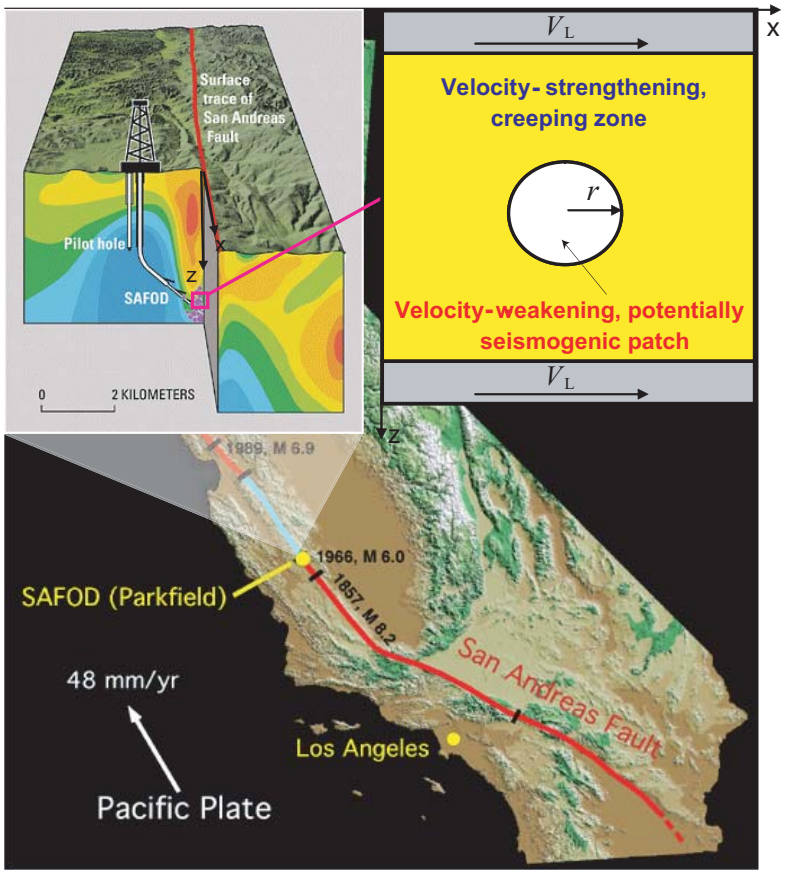

Figure 1. Schematics of the model. To simulate repeating earthquakes, such as the targets of SAFOD drilling project on the Parkfield segment (shown in blue) of the San Andreas fault, we consider a segment of a vertical strike-slip fault embedded into an elastic medium and governed by rate and state friction laws. On the fault, a small, potentially seismogenic, patch with steady state velocity-weakening properties (shown in white) is surrounded by a creeping, velocity-strengthening segment (shown in yellow). Outside of the simulated fault segment, steady sliding is imposed with the long-term slip velocity V_L.

where σ is the normal traction, p is the pore pressure, f_o, V_o, a, b, and L are rate and state parameters, with L being the characteristic slip for state variable evolution, and V_c is the cut-off velocity of the order of 10^{-8} m/s. In these laws, the rate and state features result in small variations (of the order of 1-10%) from the baseline frictional strength given by $\bar{\sigma} f_o$. Despite being small, these variations are fundamentally important for physically and mathematically meaningful stability properties of frictional sliding (e.g., Rice, Lapusta, and Ranjith, 2001). Eqns (1) also give several proposed forms for the state variable evolution, the aging law, the slip law, and Kato-Tullis law, respectively. Which of these laws does a better job of representing the range of available experimental results and serves as the best simplified representation of the state variable evolution for simulations of long-term slip is an active area of research (Kato and Tullis, 2001; Hori et al., 2004; Rubin and Ampuero, 2005; Bayart et al., 2006; Ampuero and

Rubin, 2008). We have studied the behavior of the model with all these laws, with most simulations done with the aging form. We have also started to explore the behavior of the model with enhanced dynamic weakening during seismic slip, as discussed further in the following.

Spontaneous long-term slip history of fault slip is determined in this model using the 3D simulation methodology of Lapusta and Liu (2009), which is the extension of the 2D methodology of Lapusta et al. (2000). The methodology incorporates slow tectonic-type loading and all dynamic effects of self-driven dynamic rupture. The algorithm allows us to treat accurately long deformation histories and to calculate, for each earthquake episode, initially quasi-static accelerating slip (nucleation process), the following dynamic rupture break-out and propagation, postseismic response, and ongoing slippage throughout the loading period in creeping fault region. There are no kinematic assumptions in our model other than the steady slip of the creeping fault far from the location of the repeating earthquake.

As predicted by studies of stability of frictional sliding (Rice and Ruina, 1983; Dieterich, 1992; Rice et al., 2010; Rubin and Ampuero, 2005), most of the velocity-strengthening part of the fault in our model accumulates slip through steady sliding with the imposed long-term slip rate V_L. The behavior of the velocity-weakening patch depends on its radius *r*, consistent with the findings of stability studies that a sufficiently large velocity-weakening region is required for unstable slip. For sufficiently small values of *r*, the velocity-weakening patch accumulates slip through perturbed but aseismic sliding, with slip velocities that never deviate too much from the long-term slip velocity V_L. Velocity-weakening patches of larger sizes produce repeating earthquakes. For the aging formulation, the critical patch radius is well-approximated by the estimate of Rubin and Ampuero (2005) with a 3D correction (Chen and Lapusta, 2009).

As shown in previous USGS-supported studies, the model with the standard rate and state friction (eqn. 1) is capable of reproducing the observed scaling $T \sim M_0^{0.17}$ (Nadeau and Johnson, 1998) between the recurrence time *T* and the seismic moment M_0 (Chen and Lapusta, 2009; Chen and Lapusta, 2011) for a wide range of models including several forms of state variable evolution (with important differences discussed in the previous report), different shapes of patches, and quasi-dynamic simulations.

The ability of the model to reproduce the observed non-trivial response to accelerated creeping rates

To further test and improve our model, we have applied it to simulate the response of small repeating earthquakes to accelerated loading due to postseismic slip after the M6 2004 event (Chen et al., 2010). The analysis of 34 repeating earthquake sequences (RES) from 1987 to 2009 at Parkfield shows that, following the 2004 M6 earthquake, many of the repeating events had greatly reduced recurrence intervals *T* that systematically increased with time after the 2004 event. This expected behavior of the recurrence time is easily reproduced by our model.

However, in addition to this change in timing, observations also point to systematic changes in seismic moment M_0, with some sequences experiencing significant increase in seismic moment due to higher loading rates (and hence shorter recurrence times), while other sequences have a small decrease (Figure 2). The latter behavior is what one would expect based on shorter recurrence time and laboratory-based ideas of strengthening in stationary contact (e.g., Beeler et al., 1994; Marone, 1998).

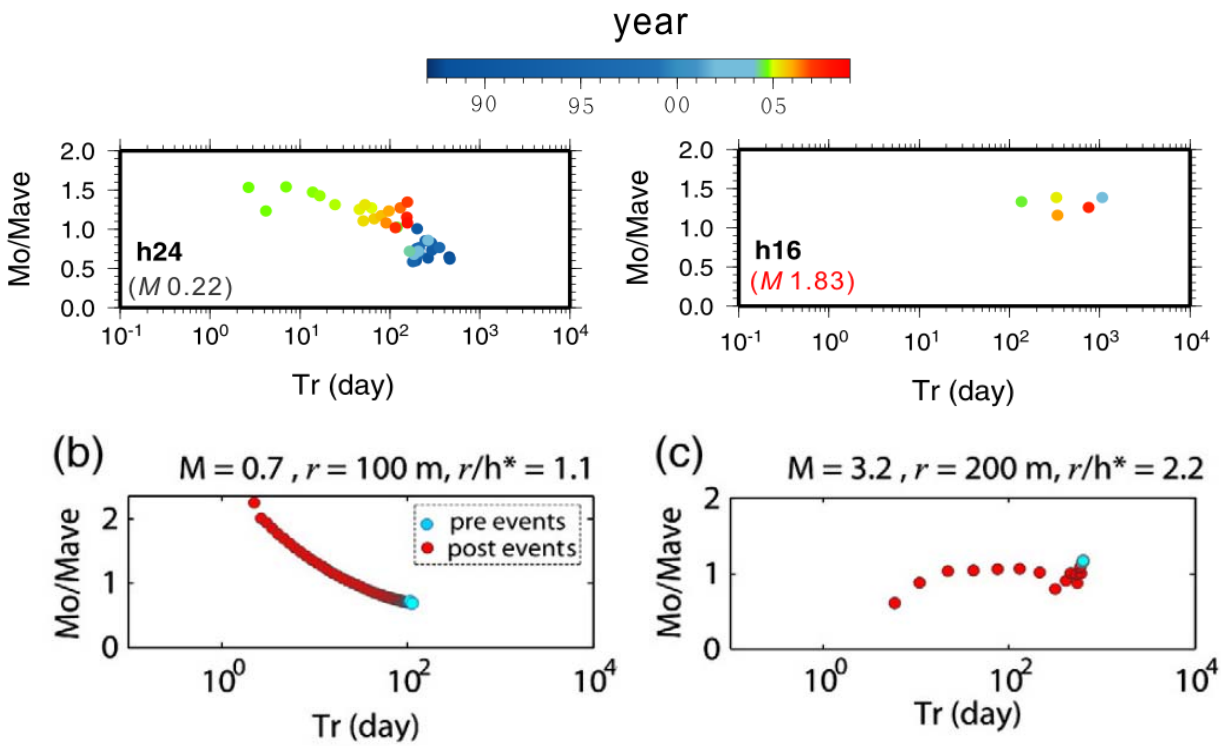

Figure 2. Response of repeating earthquakes to accelerated creep due to the 2004 earthquake. Top: Observations for two repeating sequences. Blue colors indicate repeating earthquakes before the 2004 event, and green to red colors indicate repeating earthquakes after the 2004 event. Notice that sequence h24 has larger moments for shorter recurrence times, whereas sequence h16 has nearly constant moments. Bottom: Results of our simulations with variable loading rate mimicking postseismic slip of the 2004 event. Blue and red indicate events before and after 2004, respectively. The model qualitatively matches the observed behavior, with the different dependence of the moment on the recurrence time for different values of r/h^*. Modified from Chen et al. (2010).

Our model is capable of reproducing both behaviors (Figure 2), for different sizes of the earthquake patches as quantified by the ratio r/h^* of patch size r to the nucleation size estimate h^*. Ratios of $r/h^* \sim 1$ produce higher moments M_0 for shorter recurrence times T (or negative M_0 vs. T slopes), whereas larger ratios of r/h^* yield weak positive slopes. In our models, such variations in seismic moment are caused by the fact that, for $r/h^* \sim 1$, only part of the velocity-weakening patch is ruptured seismically by the event (Figure 3), with most of the slip occurring on the patch aseismically. When the loading rate is increased, the creeping rate on the velocity-weakening patch is also increased, resulting in higher stress levels and enabling seismic events to propagate farther into the patch. This increase in the rupture area creates events with larger moments for shorter recurrence times. For larger ratios of r/h^*, seismic events rupture the entire patch at all loading rates, and hence the rupture area does not vary appreciably. Then the expected effect based on fault strengthening takes over and creates ruptures with smaller moment for smaller recurrence times.

In the context of our model, the repeating sequences that exhibit increase of the moment for shorter recurrence time occur on patches that are comparable to the critical size. Hence many

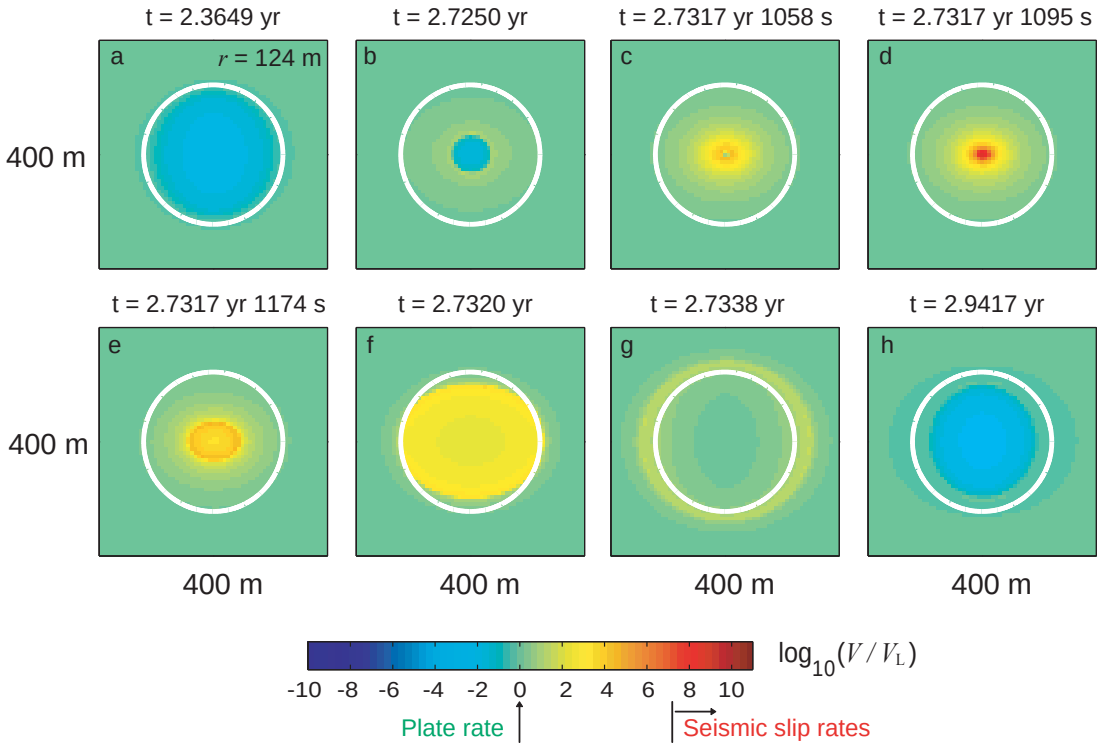

Figure 3. Snapshots of slip velocity distribution for one earthquake cycle. The size r of the patch is only slightly larger than the critical size h^* for unstable slip. Slip velocity is color coded on the logarithmic scale. The seismic range of slip velocities is indicated by red, and slip velocities close to the long-term slip velocity are indicated by green. The location of the patch is outlined by a white circle. Note that in this simulation, the extent of seismic slip is smaller than the size of the patch.

patches in Parkfield could be just at the right size to produce seismic events. This explains why some of them exhibit periods of quiescence, since small changes in their properties could make them sub-critical and hence completely aseismic. This also implies that many repeaters in Parkfield occur on patches that accumulate most of their slip seismically. Note that in our model, seismic events that rupture only a part of the velocity-weakening patch robustly occur only for the aging from of the state variable evolution. Such events are important for matching the observations discussed here, as it enables significant variations in rupture area under different loading conditions. However, similar behavior may result for heterogeneous patches or for patches with a constitutive response that incorporates a stabilizing factor such as dilatancy (e.g., Segall and Rice, 1995).

Given the same nucleation size h^* (i.e., the same frictional properties and effective normal stress), smaller radii and hence smaller seismic moments result in negative M_0 vs. T slopes, whereas larger radii and hence larger moments lead to weak positive M_0 vs. T slopes. The hints of such dependence are present in observations (Chen et al., 2010). Note that the dependence can be obscured by variations in friction properties and effective normal stress, which would result in variations in h^*. Such variations can make repeaters of a similar average moment have different r/h^* and hence different response to increased loading rates.

Note that the rate-and-state friction law used in our model incorporates fault strength recovery in stationary contact observed in the lab (Dieterich, 1972; Beeler et al., 1994; Marone, 1998). Yet the model does not automatically result in increasing moment with increasing recurrence time. This is because suggestions that fault strength recovery should lead to increase of M_o with increasing T (Vidale et al., 1994; Schaff et al., 1998) are based on simple models that envision earthquake-producing patches reaching static strength over their entire area, as would occur in a single-degree-of-freedom spring-slider approximation. However, the response of the 3D continuum model used in this study is governed by complex multiple-degree-of freedom interactions, with stress concentrations at the boundaries between creeping and locked regions and combinations of seismic and aseismic slip on the earthquake-producing patches. Hence the presence of fault strength recovery does not lead to easily predictable results, and indeed produces both positive and negative trend of M_o with T, depending on the ratio r/h^*.

Enhancing co-seismic weakening is needed to match properties of the LA and SF repeaters

The success of the model in reproducing observations indicates that such a model - with laboratory-motivated friction response and parameters - can be applied to explain observations of fault slip, with no additional scaling. This important finding obtained with USGS support is quite encouraging. It has motivated us to apply the model to the two well-studied repeaters, the LA and SF sequences (Figure 4), with the goal of applying it to understand slip phenomena at Parkfield not only qualitatively but also quantitatively.

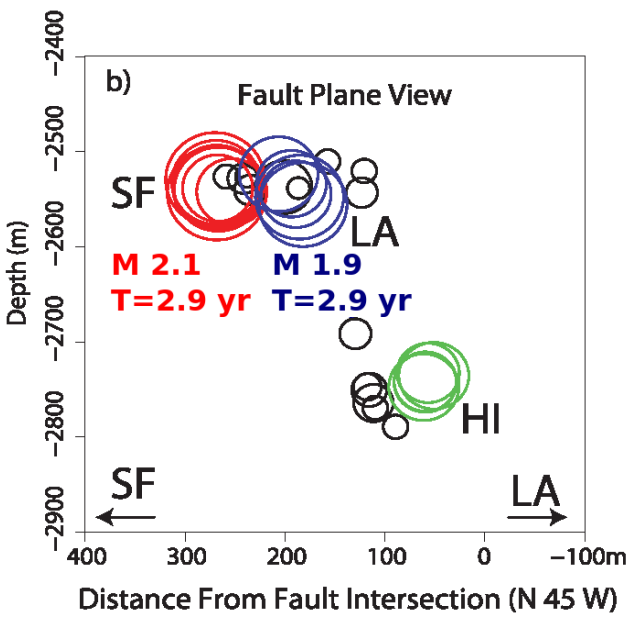

Figure 4. The SF and LA sequences are located close to each other, separated by only about 60-70 m along strike (e.g., Zoback et al., 2010). The SF sequence has the average moment magnitude of M2.1, a concentrated circular slip area of about 40 m in diameter, average stress drop over the areas of positive slip of 10-20 MPa and local stress drops as high as 60 MPa (Dreger et al., 2007) . The LA sequence has the average magnitude of M1.9. The recurrence times for both sequences are about 2.9 years. LA sequence events tend to occur within 24 hours after SF sequence events, suggesting a triggering effect (Nadeau et al., 2004). Modified from Zoback et al., 2010.

SAFOD seismic records have enabled determination of stress drops in small repeating earthquakes, with reported values reaching 30 MPa and even being as high as 60-90 MPa locally (e.g., Imanishi and Ellsworth, 2010; Dreger et al., 2007; Abercrombie et al., 2010). With the effective normal stress of 100 MPa, such stress drops imply dynamic changes in friction coefficient of 0.3, and perhaps as high as 0.6 to 0.9. Such seismic observations imply the following:

(1) The static (slow-slip) friction coefficient in the velocity-weakening patches has to be high enough to allow for such stress drops. Hence typical values of 0.6 found for velocity-weakening rock surfaces in the lab should be relevant for at least some seismogenic patches within the creeping Parkfield segment. This means that the seismogenic patches and creeping regions differ in their static (low-velocity) friction coefficients, since recent laboratory studies on the actual fault samples from SAFOD indicate that the creeping segment at the SAFOD drilling site is weak due to the presence of special minerals (Lockner et al, 2011; Jeppson et al., 2010; Holdsworth et al., 2011). The friction coefficients found in the lab are as low as 0.15. The potential difference in static friction coefficients between creeping and seismogenic regions is not surprising since the regions are already different in terms of producing stable vs. unstable slip.
(2) The co-seismic change in friction coefficients implied by the high stress drops is well beyond the range of changes possible in the logarithmic formulations such as Egn. 1. Hence we need to incorporate more significant weakening mechanisms that get activated at fast, seismic slips.

These two inferences, taken together, suggest that at least some patches that produce small repeating earthquakes are statically strong but dynamically weak. Large-scale faults with such properties are expected to operate under low levels of stress (e.g., Lapusta and Rice, 2004). However, because these patches are small - only slightly (1-3 times) larger than their nucleation sizes – the patches have to be well-stressed over much of their area to nucleate seismic slip. That is why they operate at the level of stress close to their (high) static strength and can experience large stress drops.

Our prior support from USGS and NSF has enabled us to incorporate shear heating dynamic weakening mechanisms, such as flash heating and thermal pressurization, into our simulations of earthquake cycles (e.g., Noda and Lapusta, 2010). One shear-heating weakening mechanism that has laboratory support is flash heating (e.g., Rice, 1999, Goldsby and Tullis, 2003, Beeler and Tullis, 2003, Rice, 2006, Beeler et al. 2007), in which tips of contacting fault gouge grains heat up and weaken. Such weakening can be activated even for very small slips of the order of 10-100 microns if the shear strain rate is high enough. Hence this mechanism can be important even for the smallest repeating earthquakes. Another relevant mechanism is pore fluid pressurization (e.g., Sibson, 1973; Lachenbruch, 1980; Mase and Smith, 1987; Andrews, 2002; Noda, 2004; Bizzarri and Cocco, 2006a,b; Rice, 2006; Noda et al., 2009).

Variations in shear localization that leads to flash heating and/or variations in hydraulic properties between different seismogenic patches could contribute to the observed significant differences between their source properties (e.g., Imanishi and Ellsworth, 2010). Furthermore, significant feedback between the seismic process and enhanced dynamic weakening (that tends to be strongly rate-dependent) would create differences between earthquakes in the same repeating sequence, potentially leading to behaviors that do not fit into simplified slip-predictable or time-predictable models. This is precisely what is observed at Parkfield (e.g., Rubinstein et al., 2010).

To include flash heating and/or pore pressurization into our models, we modify the logarithmic rate and state formulation (1) to

$$\tau_f = \bar{\sigma} f = (\sigma - p)\left[\frac{f_o - f_w + a\ln(V/V_o) + b\ln(V_o\theta/L)}{1 + L/\theta V_w} + f_w\right], \tag{4}$$

where V_w is the characteristic slip velocity at which flash heating starts to operate, f_w is the residual friction coefficient, and pore pressure p could be evolving due to shear heating as discussed below. Based on laboratory experiments and flash heating theories, V_w is of the order of 0.1 m/s. Selecting much larger values of V_w would effectively disable the additional weakening due to flash heating. The coupled temperature and pore pressure evolution is calculated by (Rice, 2006 and references therein, Noda et al., 2009, Noda and Lapusta, 2010):

$$\frac{\partial T}{\partial t} = \alpha_{th} \frac{\partial^2 T}{\partial y^2} + \frac{\omega(y)}{\rho c}, \quad \frac{\partial p}{\partial t} = \alpha_{hy} \frac{\partial^2 p}{\partial y^2} + \Lambda \frac{\partial T}{\partial t}, \tag{5}$$

where y is the space coordinate normal to the fault, T is the temperature, α_{th} and α_{hy} are the thermal and hydraulic diffusivities, $\omega(y)$ is the heat generation rate the integral of which equals to $\tau_f V$, ρc is the specific heat, Λ is pore pressure change per unit temperature change under undrained condition. (Note that this formulation can also include inelastic dilatancy, as an additional term in the equation for the pore pressure evolution.) The heat source, $\omega(y)$, is distributed in a narrow shear zone around the fault. The standard assumption is to take this term to represent the effect of uniform sliding in the fault zone of half width w.

Our modeling of the LA and SF repeaters indeed shows enhanced co-seismic weakening is required to reproduce the observed magnitude, rupture area, and stress drop of the two sequences. Our preferred model is shown in Figure 5, with a M2 event triggering a M1.9 event after about 2 hours in the instance shown. The model consists of two circular velocity-weakening patches surrounded by large velocity-strengthening region. The centers of the two patches are separated by 60 m to match the seismic observations on the distance between the hypocenters of LA and SF repeaters. The patch for the SF repeaters is set to be a littler larger (r_1 = 20 m) than the patch for the LA repeaters (r_2 = 15 m) considering that the SF repeaters have larger magnitudes (M2.1) than the LA repeaters (M1.9). The effective normal stress of 120 MPa (consistent with observations in the area) and enhanced dynamic weakening are used to match seismic observations of high stress drops for these repeaters. Our simulated average stress drops in this model are 10 to 20 MPa, and local stress drops can reach as high as 60 to 80 MPa, similar to seismic observations. Based on our simulations, if two closely separated patches have similar patch sizes and nucleation sizes, it is more likely that a smaller earthquake triggers a larger earthquake. To account for the observations that the larger SF repeaters usually trigger the smaller LA repeaters, we make the patch for the SF repeaters have smaller nucleation size ($2h_1^*$ = 9 m, $r_1/h_1^* \approx 4$) than the patch for the LA repeaters ($2h_2^*$ = 56 m, $r_2/h_2^* \approx 0.5$) by assigning different characteristic slip values (L_1 = 20 μm, L_2 = 120 μm). Pore pressurization weakening is used in this model, and the parameters values are: $\alpha_{th} = 10^{-6}$ m^2/s, w = 0.5 mm everywhere, a = 0.015, b = 0.019, $\alpha_{hy} = 10^{-4}$ m^2/s, Λ = 1 MPa/K in the velocity-weakening patches, and a = 0.019, b = 0.015, $\alpha_{hy} = 10^{-2}$ m^2/s, Λ = 0 MPa/K in the velocity-strengthening region. In this model, the patch for the LA repeaters is smaller than the nucleation size and hence it cannot nucleate seismic events by itself. After an event on the SF patch, the LA patch can be triggered through interaction with the SF events. The triggering time depends on the instantaneous stress change, post-seismic slip imposed by the SF events, and the nucleation process on the LA patch.

Our preferred model, shown in Figure 5, successfully reproduces the hypocenter separation distance, rupture area, magnitude, stress drops, triggering order, and triggering time of

the LA and SF repeaters as observed. The recurrence times have not yet been explored in this model, as only several events in the sequence have been simulated for various selections of physical properties, but this issue will be more fully explored in future work. Our proposed model is only one of the models that could explain the observations, and exploring the space of suitable parameters is another topic for future work. However, the model highlights some important ingredients such as high effective normal stress and enhanced dynamic weakening, adds insights into the interaction between the LA and SF sequences, and provides a way to integrate future observations about these sequences. One of the issues to be explored in the future work is the source of the observed variability in the recurrence and triggering times for the LA and SF repeaters.

Interaction of two potentially seismogenic patches

As part of our modeling of the LA and SF repeaters, we have started a systematic investigation of the interaction of two nearby seismogenic patches using a 2D in-plane model (Figure 6a) instead of the full 3D model for computational efficiency. In the model, the distance between the centers of the two potentially seismogenic patches is fixed to be 60 m as observed for the LA and SF repeaters. The half nucleation size is 12 m for both patches. Models with different sizes of the two patches produce qualitatively different interaction between the patches. For example, when the two patches are both about the nucleation size, each patch is seismically active for a certain period of time while the other patch is quiescent, and then the roles of the patches switch (Figure 6b). When the two patches are of the same size which is slightly larger than the nucleation size, a seismic event on one patch triggers a larger event that nucleates on the other patch and ruptures both patches (Figure 6c). When one of the patches is smaller than the nucleation size and the other patch is larger than the nucleation size, a seismic event on the larger patch triggers seismic slip on the smaller patch which would be totally aseismic in isolation (Figure 6d). However, triggering does not always promote more seismic response. For example, when one patch is slightly larger than the nucleation size and hence would be expected to rupture seismically in isolation, seismic events on the other even larger patch could inhibit seismic slip on the smaller patch by inducing aseismic slip there (Figure 6e). The rich range of behaviors for two nearby velocity-weakening patches suggested by our simulations highlights the importance of accounting for the interaction of the nearby repeaters and shows that the resulting behavior is not always what one would intuitively expect.

Our simulations so far suggest that much of the interaction between seismic events in the two sequences occurs through accelerated post-seismic creep in the areas between potentially seismogenic regions, and not simply through direct static (or dynamic) stress changes imposed by one event on the location of the other event. Such creep-mediated stress changes introduce additional time scales into the problem, and make the triggering time dependent not only on the nucleation process and instantaneous stress changes, but also on the properties of post-seismic slip and its propagation.

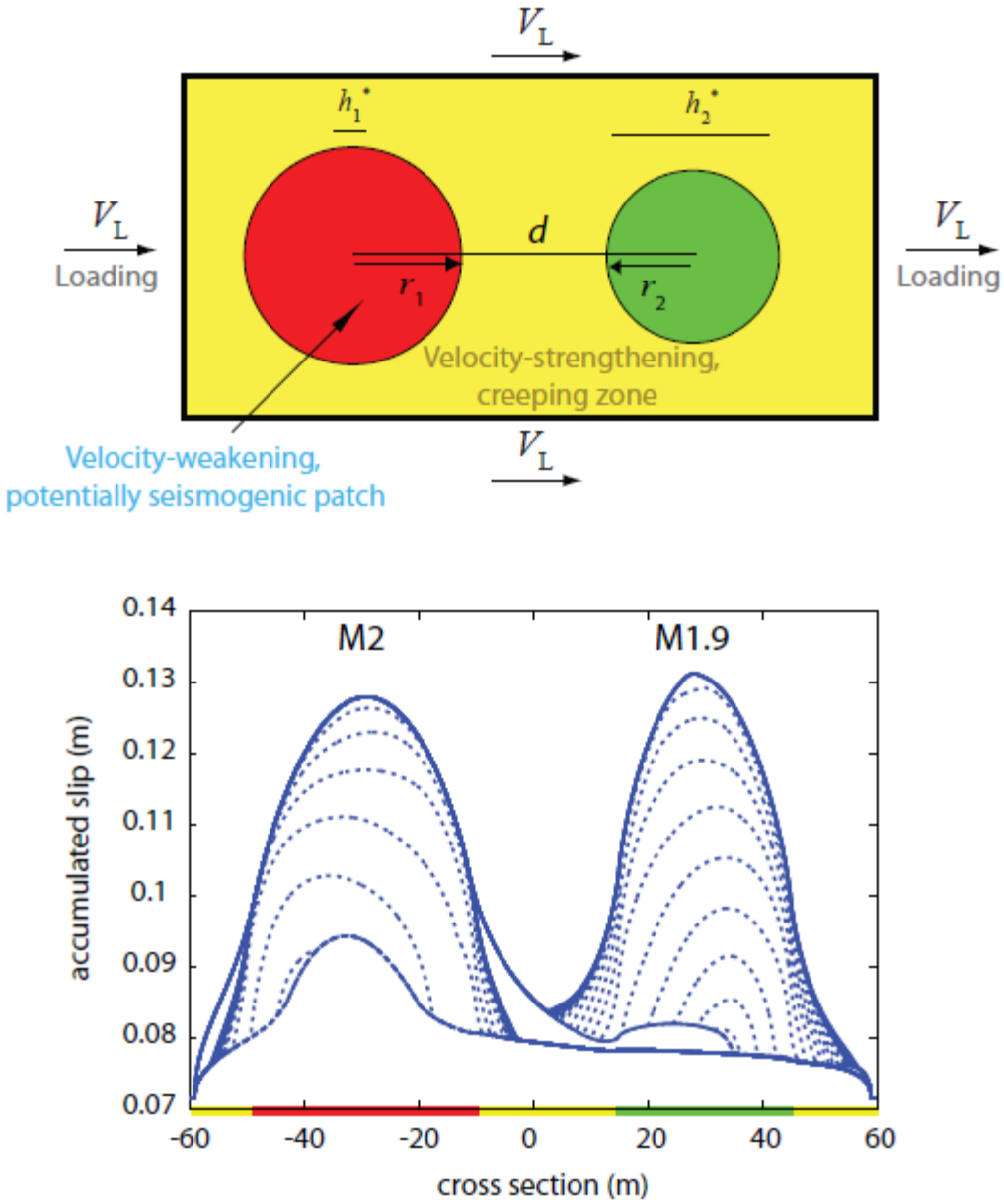

Figure 5. Two patches in our model interact in a way similar to the SF and LA sequences. Top: Two velocity-weakening patches (r_1 = 20 m, r_2 = 15 m, d = 60 m) with enhanced dynamic weakening, embedded into a creeping section. The creeping section shown here is only part of the wider creeping zone used in the model. Half nucleation sizes h_1^* and h_2^* for the two patches are shown for scale. Bottom: The simulated response for one cycle. Seismic slip profile along the cross section is shown for every 0.001 second (blue lines). The locations and sizes of the two patches and creeping zone are illustrated with color at the bottom. During this cycle, the left patch produces M2 that triggers M1.9 on the right patch, about 2 hours later, similar to observations.

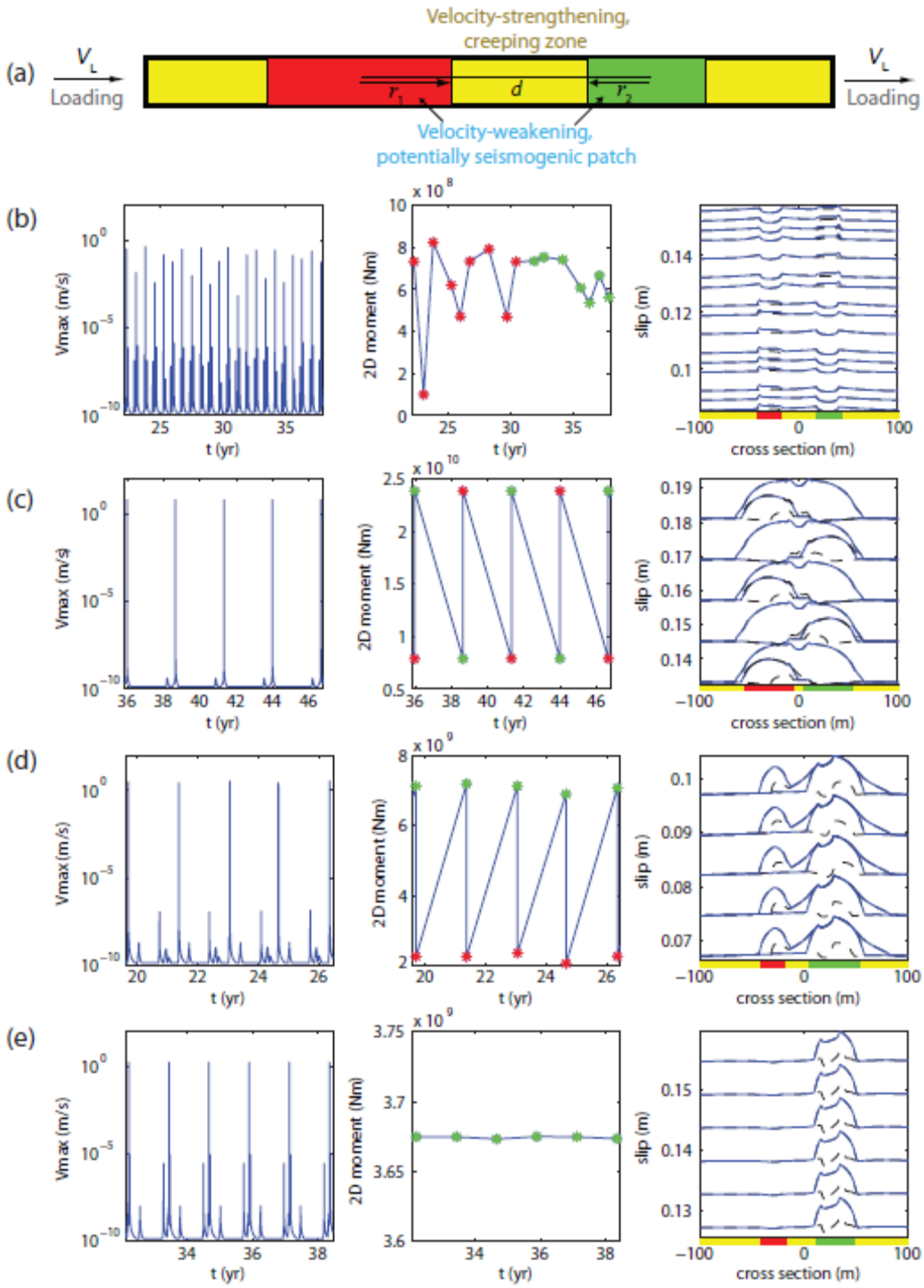

Figure 6. Examples of interaction between two potentially seismogenic patches embedded into a creeping region. (a) 2D in-plane model with two patches. (b-e) A selection of simulation results with the same separation distance (d = 60 m) and half nucleation size (h^* = 12 m) but different patch sizes: (a) $r_1 = 1\ h^*$, $r_2 = 1\ h^*$, (b) $r_1 = 2\ h^*$, $r_2 = 2\ h^*$, (c) $r_1 = 0.95\ h^*$, $r_2 = 2\ h^*$, (d) $r_1 = 1.02\ h^*$, $r_2 = 1.5\ h^*$. The left panels show the maximum slip velocity on the fault vs. time. Spikes represent either seismic events (if Vmax > 0.01 m/s) or aseismic transients (if Vmax < 0.01 m/s). The middle panels show the seismic moment per unit

width of the 2D fault for each seismic event vs. time. Red and green stars indicate seismic events that mostly rupture the left and right patch, respectively. The right panels show slip profiles along the fault before (black dashed line) and after (blue solid line) each seismic event. The locations and sizes of patches are drawn at the bottom for reference. See the text for more details on the simulated behaviors.

References

Abercrombie, R. E. (1995), Earthquake source scaling relationships from -1 to 5 M_L using seismograms recorded at 2.5-km depth, *J. Geophys. Res*., **100**, 24,015– 24,036.

Allmann, B. P., and P. M. Shearer, Spatial and temporal stress drop variations in small earthquakes near Parkfield, California, *J. Geophys. Res*., **112**, B04305, doi:10.1029/2006JB004395, 2007.Ampuero, J.-P., and A. M. Rubin, Earthquake nucleation on rate and state faults-Aging and slip laws, J. Geophys. Res., 113, B01302, doi:10.1029/2007JB005082, 2008.

Andrews, D. J., A fault constitutive relation accounting for thermal pressurization of pore fluid, *J. Geophys. Res.*, **107**(B12), 2363, doi:10.1029/2002JB001942, 2002.

Bayart, E., A. M. Rubin, and C. Marone, Evolution of Fault Friction Following Large Velocity Jumps, *Eos Trans. AGU*, **87**(52), Fall Meet. Suppl., S31A-0180, 2006.

Beeler, N. M., T. E. Tullis, and J. D. Weeks , The roles of time and displacement in the evolution effect in rock friction, *Geophys. Res. Lett*., **21**, 1987–1990, 1994.Beeler, N. M., D. L. Lockner, and S. H. Hickman, A simple stick-slip and creep-slip model for repeating earthquakes and its implication for microearthquakes at Parkfield, *Bull. Seismol. Soc. Am*., **91**, 1797– 1804, 2001.

Beeler, N. M., and T. E. Tullis, Constitutive relationships for fault strength due to flash-heating. In: *2003 SCEC Annual Meeting Proceedings and Abstracts*, vol. 13, p. 66. Los, Angeles: Southern California Earthquake Center, Univ. of Southern California, 2003.

Beeler, N. M., T. E. Tullis, and D. L. Goldsby , Constitutive relationships and physical basis of fault strength due to flash-heating, *J. Geophys. Res*., **113**, B01401, doi:10.1029/2007JB004988, 2008.

Bizzarri, A., and M. Cocco, A thermal pressurization model for the spontaneous dynamic rupture propagation on a three-dimensional fault: 1. Methodological approach, *J. Geophys. Res*., **111**, B05303, doi:10.1029/2005JB003862, 2006a.

Bizzarri, A., and M. Cocco, A thermal pressurization model for the spontaneous dynamic rupture propagation on a three-dimensional fault: 2. Traction evolution and dynamic parameters, *J. Geophys. Res*., **111**, B05304, doi:10.1029/2005JB003864, 2006b.Bürgmann, R., D. Schmidt, R. M. Nadeau, M. d'Alessio, E. Fielding, D. Manaker, T. V. McEvilly, and M. H. Murray, Earthquake potential along the northern Hayward fault, California, *Science*, **289**, 1178– 1182, 2000.

Chen, K. H., R. M. Nadeau, and R.-J. Rau, Towards a universal rule on the recurrence interval scaling of repeating earthquakes?, *Geophys. Res. Lett*., **34**, L16308, doi:10.1029/2007GL030554, 2007.

Chen, K. H., R. Bürgmann, R. M. Nadeau, T. Chen, and N. Lapusta, Postseismic variations in seismic moment and recurrence interval of repeating earthquakes, *Earth Planet. Sci. Lett*., 299 (1-2), 118 – 125, doi:10.1016/j.epsl.2010.08.027, 2010.

Chen, T., and N. Lapusta , Scaling of small repeating earthquakes explained by interaction of seismic and aseismic slip in a rate and state fault model, *J. Geophys. Res.*, 114, B01311, doi:10.1029/2008JB005749, 2009.

Chen, T., and N. Lapusta, Interaction of small repeating earthquakes in a rate and state fault model, *SCEC annual meeting*, 2010,

Chen, T., and N. Lapusta, Interaction of small repeating earthquakes in a rate and state fault model, Abstract T33B-2255, *AGU Fall Meeting*, 2010,

Dieterich, J. H., Modeling of rock friction- 1 Experimental results and constitutive equations, *J. Geophys. Res.*, **84**, 2161-2168, 1979.

Dieterich, J. H., Constitutive properties of faults with simulated gouge, in *Mech. Beh. Crustal Rocks*, Geophys. Monogr. Ser., **24**, ed. by N. L. Carter, M. Friedman, J. M. Logan and D. W. Stearns, AGU, Washington, DC, 103-120, 1981.

Dieterich, J. H., Earthquake nucleation on faults with rate-dependent and state-dependent strength, *Tectonophysics*, **211**, 115–134, 1992.Dreger, D., R. M. Nadeau, and A. Chung, Repeating earthquake finite source models: Strong asperities revealed on the San Andreas fault, *Geophys. Res. Lett*., **34**, L23302, doi:10.1029/2007GL031353, 2007.

Ellsworth, W. L. and L. D. Dietz, Repeating earthquakes: characteristics and implications, Proc. of Workshop 46, the 7th U.S.-Japan Seminar on Earthquake prediction, U.S.Geol.Surv. Open-File Rept. 90-98, 226-245, 1990.

Goldsby, D. L., and T. E. Tullis, Flash heating/melting phenomena for crustal rocks at (nearly) seismic slip rates. In: *2003 SCEC Annual Meeting Proceedings and Abstracts*, vol. 13, p. 98-99. Los Angeles: Southern California Earthquake Center, Univ. of Southern California, 2003.

Hickman, S., M. Zoback, and W. Ellsworth, Introduction to special section: Preparing for the San Andreas Fault Observatory at depth, *Geophys. Res. Lett*., **31**, L12S01, doi:10.1029/2004GL020688, 2004.

Holdsworth, R. E., E. W. E. van Diggelen, C. J. Spiers, J. H. P. de Bresser, R. J. Walker, and L. Bowen, Fault rocks from the SAFOD core samples: Implications for weakening at shallow depths along the San Andreas Fault, California, *Journal of Structural Geology,* **33,** 132-144, 2011.

Hori, T., N. Kato, K. Hirahara, T. Bada, and Y. Kaneda, A numerical simulation of earthquake cycles along the Nankai trough, southwest Japan: Lateral variation in frictional property due to slab geometry controls the nucleation position, *Earth. Planet. Sci. Lett.*, 228, 215-226, 2004.

Igarashi, T., Matsuzawa, T., and A. Hasegawa, Repeating earthquakes and interplate aseismic slip in the northeastern Japan subduction zone, *J. Geophys. Res.* 108, B5, 2249, 2003.

Imanishi, K., W. L. Ellsworth, S. G. Prejean, Earthquake source parameters determined by the SAFOD Pilot Hole seismic array, *Geophys. Res. Letters*, **31**, L12S09, doi:10.1029/2004GL019420, 2004.

Imanishi, K. and W. L. Ellsworth, Source properties of microearthquakes revealed by near-source observation at SAFOD, Abstract T52B-02, AGU Fall Meeting Abstracts, 2010.

Jeppson, T. N., K. K. Bradbury, and J. P. Evans, Geophysical properties within the San Andreas Fault Zone at the San Andreas Fault Observatory at Depth and their relationships to rock properties and fault zone structure, *J. Geophys. Res.*, **115**, B12423, 2010.

Kato, N., and T. E. Tullis, A composite rate- and state-dependent law for rock friction, *Geophys. Res. Lett.*, 28, 1103–1106, 2001.

Lachenbruch, A. H. and J. H. Sass, Heat flow and energetics of the San Andreas fault zone, *J. Geophys. Res*., **85**, 6185-6223, 1980.

Lapusta , N., and Y. Liu, Three-dimensional boundary integral modeling of spontaneous earthquake sequences and aseismic slip, *J. Geophys. Res.*, 114, B09303, doi:10.1029/2008JB005934, 2009

Lapusta, N. and J. R. Rice, Earthquake sequences on rate and state faults with strong dynamic weakening, *Eos Trans. AGU*, 85(47), T22A-05, 2004.

Lapusta, N., J. R. Rice, Y. Ben-Zion, and G. Zheng, Elastodynamic analysis for slow tectonic loading with spontaneous rupture episodes on faults with rate- and state-dependent friction, *J. Geophys. Res*. 105, 23765-23789, 2000.

Lockner, D. A., C. Morrow, D. Moore, and S. Hickman, Low strength of deep San Andreas fault gouge from SAFOD core, *Nature*, **472**, 82-85, 2011.

Marone, C., Vidale, J. E., and W. L. Ellsworth, Fault healing inferred from time-dependent variations in-source properties of repeating earthquakes, *Geophys. Res. Lett.,* 22, 3095-3098, 1995.

Marone, C. , Laboratory-derived friction laws and their application to seismic faulting, Ann. *Rev. Earth Planet. Sci*., **26**, 643– 696, 1998.

Mase, C. W., and L. Smith, Effects of frictional heating on the thermal, hydrologic, and mechanical response of a fault, *J. Geophys. Res*., **92**, 6249– 6272, 1987.

Matsubara, M., Y. Yagi, and K. Obara, Plate boundary slip associated with the 2003 off-Tokachi earthquake based on small repeating earthquake data, *Geophys. Res. Lett*., **32**, L08316, doi:10.1029/2004GL022310, 2005.

Nadeau, R. M., and L. R. Johnson, Seismological studies at Parkfield VI: Moment release rates and estimates of source parameters for small repeating earthquakes, *Bull. Seism. Soc. Am.,* 88, 3, 790-814, 1998.

Nadeau, R. M., and T. V. McEvilly, Fault slip rates at depth from recurrence intervals of repeating microearthquakes, *Science*, **285**, 718–721, 1999.

Nadeau, R. M., A. Michelini, R. A. Uhrhammer, D. Dolenc, T. V. McEvilly, Detailed kinematics, structure and recurrence of micro-seismicity in the SAFOD target region, *Geophys. Res. Letters*, **31**, L12S08, doi:10.1029/2003GL019409, 2004.

Noda, H., Numerical simulation of rupture propagation with thermal pressurization based on measured hydraulic properties: Importance of deformation zone width, *EOS Trans. AGU* **85**(47), Fall Meeting Suppl., Abstract T22A-08, 2004.

Noda, H., E. M. Dunham, and J. R. Rice, Earthquake Ruptures with Thermal Weakening and the Operation of Major Faults at Low Overall Stress Levels, *J. Geophys. Res.*, doi:10.1029/2008JB006143, 2009.

Noda, H., and N. Lapusta (2010), Three-dimensional earthquake sequence simulations with evolving temperature and pore pressure due to shear heating: Effect of heterogeneous hydraulic diffusivity, *J. Geophys. Res*., 115, B12314, doi:10.1029/2010JB007780.

Rice, J. R., Flash heating at asperity contacts and rate-dependent friction, *Eos Trans. AGU*, **80**(46), Fall Meet. Suppl., F681l, 1999.

Rice, J. R., Heating and weakening of faults during earthquake slip, *J. Geophys. Res*., doi:10.1029/2005JB004006, 2006.

Rice, J. R., and A. L. Ruina, Stability of a steady frictional slipping, *J. Appl. Mech*., 50, 343-349, 1983.

Rice, J. R., N. Lapusta, and K. Ranjith, Rate and state dependent friction and the stability of sliding between elastically deformable solids, *J. Mech. Phys. Solids* 49, 1865-1898, 2001.

Rubin, A.M., and J.-P. Ampuero, Earthquake nucleation on (aging) rate and state faults, *J. Geophys. Res.,* 110, doi:10.1029/2005JB003686, 2005.

Rubinstein, J. L., W. L. Ellsworth, N. M. Beeler, K. H. Chen, D. A. Lockner, and N. Uchida, Except in Highly Idealized Cases, Repeating Earthquakes and Laboratory Earthquakes are Neither Time- nor Slip-Predictable, Abstract S33B-2082, AGU Fall Meeting, 2010.

Ruina, A. L., Slip instability and state variable friction laws, *J. Geophys. Res*., **88**, 10359-10370, 1983.

Sammis, C. G., and J. R. Rice, Repeating earthquakes as low-stress-drop events at a border between locked and creeping fault patches, *Bull. Seism. Soc. Am.,* 91, 3, 532-537, 2001.

Schaff, D. P., and G. C. Beroza, Coseismic and postseismic velocity changes measured by repeating earthquakes, *J. Geophys. Res*., **109**, B10302, doi:10.1029/2004JB003011, 2004.

Segall, P., and J. R. Rice, Dilatancy, compaction, and slip instability of a fluid infiltrated fault, *J. Geophys. Res*., **100**(B11), 22,155-22,171, 1995.

Sibson, R. H., Interaction between temperature and pore-fluid pressure during earthquake faulting and a mechanism for partial or total stress relief, *Nature*, **243**, 66–68, 1973.

Vidale, J. E., Ellsworth, W. L., Cole, A., and C. Marone, Variations in rupture process with recurrence interval in a repeated small earthquake, *Nature*, 368, 6472, 624-626, 1994.

Zoback, M., S. Hickman, and W. Ellsworth, Scientific Drilling Into the San Andreas Fault Zone, *Eos Trans. AGU*, **91**, 197-198, 2010.